Application of signal reconstruction techniques to shot count reduction in simulation driven fracturing

Shangliang Jiang and Avideh Zakhor

Signetron Inc. and Department of Electrical Engineering and Computer Sciences
University of California at Berkeley, CA, 94720, USA
Email: {sjiang,avz}@eecs.berkeley.edu

ABSTRACT

Traditionally, Variable Shape Electron Beam (VSEB) mask writing tools generate pixel-based optical proximity correction (OPC) or inverse lithography technology (ILT) masks by first simplifying them into a rectilinear polygon, and then partitioning the rectilinear polygon into shots. However, as these masks are complex and curvilinear, this approach results in an explosion of shot count and mask write time, and a loss of optimality of the OPC solution. In this work we propose an alternative fracturing approach to minimize mask write time in which the shot location, size, and dose are determined using the mask fabrication model. In doing so we allow shots to overlap in order to reduce the shot count while maintaining mask and wafer quality. Our approach is based on overcomplete signal expansion algorithms which have traditionally been used for sparse representation and compression of images and videos. Our simulation results on a 45nm random logic and contact hole circuit show shot count reduction by as much as 50%.

Keywords: Model-based fracturing, mask data preparation, Variable Shaped Beam mask writing

1. INTRODUCTION

Resolution enhancement techniques such as Optical Proximity Correction (OPC)[12] have enabled the semiconductor manufacturing industry to continuously shrink the critical dimension (CD) of integrated circuits. Complex pixel-based OPC shows promise in continuing this aggressive shrinkage. However, the resulting masks are complex and require excessively long write times. This is because they are curvy and hence difficult to manufacture. The current mask fabrication process with Variable Shape Electron Beam (VSEB) mask writing tools consists of (a) approximating the curvilinear shapes with a rectilinear polygon, and (b) partitioning the rectilinear polygon into rectangular or trapezoidal shots. This process results in both an explosion of shot count and loss of optimality of the OPC solution.

In this work, we propose an alternative fracturing approach to minimize mask write time, whereby the shot location, size, and dose are determined from the curvilinear OPC output. We model the resist with a fixed nonlinear threshold function and the electron beam proximity effect by convolution with a scattering filter, namely a sum of Gaussians. Furthermore, we allow for overlap of shots. With this setup we determine the shots using a greedy approximation algorithm. The algorithm is inspired by the matching pursuit algorithm typically used in image and video compression whereby a dictionary of basis functions is searched to find the position and amplitude of atoms to approximate an image.[21]

We modify the matching pursuit algorithm, originally proposed by Mallat,[9] to refine the shot dosage, position, and location at each iteration. This is inspired by early results in edge-based OPC that greedily improve the quality of the aerial image with edge movement.[12–18] After each edge movement we reevaluate the best dosage and recompute the error. After a fixed number of iterations we accept the resulting shot and repeat this greedy process to find additional shots.

In Section 2, we review past results on fracturing. We review the matching pursuit algorithm in Section 3 to motivate our proposed algorithm in Section 4. In Section 5 we provide experimental results for our proposed algorithm. We conclude with possible directions for future work in Section 6.

2. BASICS OF FRACTURING

In this section we review prior results on fracturing. Section 2.1 reviews past results on mask manufacturability, and Section 2.2 reviews recent results on model-based fracturing, in which the mask fabrication process is modeled.

2.1 Mask manufacturing quality

Bloecker et al. have evaluated many metrics to quantify fracturing quality;[4] they proposed and demonstrated that shoreline or external sliver length is a suitable metric for evaluating fracture quality as it closely correlates with manufacturability while being fast to evaluate. Features with width below a threshold δ, as determined by the VSB mask-writing tool, are called slivers. Slivers whose length is along the boundary of the layout polygon are called external slivers. As the shot size becomes smaller, the electron current density becomes steeper, adversely affecting the shot placement. Thus slivers result in large size variability, negatively affecting CD control.[3] Many existing fracturing approaches focus on reducing sliver length.[10,11]

Spence et al. have demonstrated that the number of shots is directly correlated with the write-time.[5] Furthermore, it is reasonable to assume that the shot count is approximately equal to the number of post-fracture figures, namely the resulting trapezoids from partitioning the mask. This is because for small critical feature sizes, few polygons, if any, would require more than one shot. From this it follows that the write-time is directly proportional to the number of post-fracture trapezoids and thus the minimizing the latter will minimize mask write-time.

While there are algorithms which simultaneously minimize sliver number and length along with number of shots,[1,2] they ignore the underlying physics behind the mask writing process; rather, they solve a simpler geometric partitioning problem by introducing rules to capture the manufacturing parameters. A parallel can be drawn to early work in OPC that was built upon a series of rules for corrections as opposed to incorporating exact models. Our goal in this paper is to use models in the fracturing algorithms so as to create masks with lower shot count without degrading the wafer image quality.

2.2 Model based fracturing

Model-based fracturing operates directly on the curvilinear mask resulting from Inverse Lithography Techniques (ILT)[19] or pixel-based OPC[20] rather than a rectilinear approximation of the mask; this can potentially result in a more accurate mask which ultimately leads to a better wafer image. In addition, model-based fracturing accommodates overlapping shots which can lead to a decrease in shot-count, an important goal in limiting mask cost, write-time, and fidelity.[4,5]

Recently, D2S has introduced the concept of model-based mask data preparation which simulates the electron beam (e-beam) mask writing process.[6] They place overlapping shots in such a way that the simulated mask image approximates the desired target mask. In contrast to conventional rule-based fracturing, model-based fracturing places shots based upon the models for both the mask writer and the photoresist. In doing so, not only a more realistic error function is used to evaluate the quality of the fracturing, but also shot count is lowered as shots are allowed to overlap.

A number of issues need to be addressed in designing model-based fracturing algorithms. First, the electron transfer is not exact and is instead modeled by a low-pass filter, typically Gaussian or sum of Gaussians.[7] This may imply a deconvolution step which is an inherently ill-conditioned problem. Second, the energy of the electrons is transmitted and absorbed by a chemical resist which acts as a thresholding operator in terms of what appears on the resulting mask. Thresholding is a nonlinear operator and makes the problem formulation more complex because many possible energy profiles result in the same mask. In Section 4 we describe our proposed algorithm to address some of these issues.

3. MATCHING PURSUIT OVERVIEW

Overcomplete signal expansion (OSE) algorithms are used in image and video processing for signal representation and compression.[9,21–39] Two characteristics of OSE algorithms make them attractive for the fracturing problem. First, they result in a sparse representation of a signal, which in the context of fracturing amounts to minimizing shot count. This sparse approximation can arguably be attributed to the richness and flexibility of the overcomplete dictionary with many basis functions to choose from during the approximation process. Second, the regions of support of basis functions in the dictionary are typically allowed to overlap, which in the context of fracturing corresponds to shots overlapping with each other. Examples of OSE algorithms commonly used in signal processing are matching pursuit (MP), basis pursuit, and projection pursuit.

At each iteration MP maintains a "residual", which is the difference between the target signal and the approximation. Also, it uses an over-complete set of basis functions called a dictionary to iteratively find the best match between the residual and the elements of the dictionary. The algorithm is outlined below:

```
Input: signal
Output: list of basis functions and their respective coefficients
Initialize: residual = signal
Repeat:
Find the basis function with maximum-magnitude inner product with the residual
Store the value of the inner product for later use
Update the residual by subtracting the projection of the residual onto the basis function
     from the current residual
Stop: stopping condition met (e.g., error < threshold, maximum number of iterations exceeded)
```

At each step both the approximation and the residual, which is the current approximation error, are updated and saved. Initially the residual is set to the input signal as no approximation has been made.

To add a basis function to the approximation, the algorithm computes the inner product for each possible location of each basis function. Then, it selects the basis function and location pair which has the highest correlation with the residual and stores this pair along with the value of the inner product. In other words, it finds the basis function from the dictionary that minimizes the resulting error. Finally, the residual is updated by subtracting the scaled basis function from the prior residual.

While this algorithm is effective in decomposing a signal into a set of basis functions, it accomplishes this with respect to an L_2-norm error metric. The resulting shots are significantly different from what is needed in fracturing as the error metric is completely different due to the non-linearity of the resist. However, we use matching pursuit to obtain a reasonable initial guess for the shot placement and dosage.

4. PROPOSED ALGORITHM

We quantify the shot placement with two error metrics. The first is the number of shots which relates to minimizing the write time, as stated in Section 2.1. This is achieved by using a modification of matching pursuit which implicitly minimizes shot count. The second metric is the error between the simulated mask and the target mask, related to the quality of the fracturing. Rather than simply using the difference, we recognize there can be ϵ error in the placement of the contours – in particular, the edges of the simulated mask may actually fall up to ϵ distance away from the desired mask edges. Because of this, we expand the desired contour into a buffer region of width 2ϵ. Any differences between the simulated mask and the target mask within this buffer region is ignored.

As we are using a modification of matching pursuit, we require a dictionary of possible basis functions corresponding to possible shot sizes and types. In this work we only include rectangular shots. Furthermore, rather than including all possible shot sizes and locations, we prune it to only contain rectangles whose edge lengths are multiples of a parameter, called Δ. Next, each rectangular shot in the dictionary is passed through the forward scattering model, $g_f(x)$, a single 2-D Gaussian filter, shown in Equation 1, with σ_f being the forward scattering parameter:

$$g_f(x) = \frac{1}{\pi\sigma_f^2}\exp(\frac{x^2}{\sigma_f^2}) \tag{1}$$

In this work we set $\sigma_f = 30$nm. The energy profiles of the shots after the scattering filter make up our final dictionary of basis vectors. While our simulations only incorporate forward scattering, we can modify this step to allow for a more complex e-beam model.

A final requirement of matching pursuit is to compute a residual, the current error in the approximation. Normally in matching pursuit the residual is set to the difference between the target signal and the current approximation. While this is suitable for signal compression applications where the L_2 norm is minimized, it needs to be appropriately modified in the fracturing algorithm to take into account the inherent resist nonlinearity.

The dictionary of shots does not contain all possible valid shots as that would necessitate a very large dictionary resulting in an intractable runtime. To allow for any shot size to be used, we incorporate a post-processing step, similar to edge-based OPC,[12–18] that refines shot placement and sizing without increasing the dictionary size.

5. EXPERIMENTAL RESULTS

In this section we describe simulation results of our proposed MP based algorithm. We test two portions of the Metal 1 layer of a 45nm SRAM chip. A flowchart demonstrating our test setup is shown in Fig. 1. In the flow chart we refer to assist features as SRAFs. We start with the target wafer image and run PIXBar™ on it. From the resulting mask we extract the curvy assist features. We consider three assist feature types – the "raw" assist feature, a simplified assist feature, and the approximation generated by our proposed algorithm. Next, we optimize the main feature using edge-based OPC with all three kinds of assist features. This gives us three different assist feature-main feature pairs to compare the fracturing results and wafer qualities. For the raw and simple assist features we fracture the entire layout using the Calibre© fracturing software. For the output of our proposed algorithm, we generate the fracturing of the assist features from our proposed algorithm but use Calibre© to fracture the main feature. As the main feature is generated using edge-based OPC, it is more readily decomposed by traditional fracturing techniques.

Finally, we compare the shot count of the fracturing resulting from our algorithm with that of the simplified mask as determined by Calibre©. We also use wafer-level metrics to quantify our fracturing algorithm. The choice of the metric depends on our test layout and are discussed below in Sections 5.1 and 5.2.

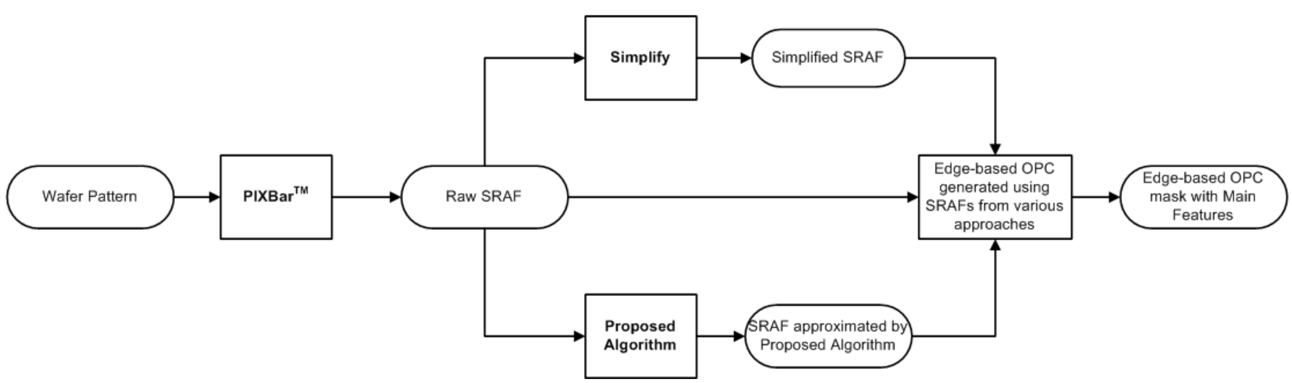

Figure 1: Flowchart describing our test setup.

Table 1: Wafer simulation conditions.

Parameter	Conditions
NA	0.95
Source	Annular, $\sigma_{in} = 0.4, \sigma = 0.7$
Mask	Chrome on glass
Resist	Ideal threshold

5.1 Random Logic

The first data set from the 45nm chip is a 5μm by 10μm random logic circuit shown in Fig. 2 (a). The widths of the polygons in the layout range from 80nm to 400nm. We provide the wafer image simulation conditions in Table 1.

Fig. 2 (b) shows the raw assist features with edge-based OPC main features. Fig. 3 shows a comparison of the three types of masks. We note that our proposed algorithm results in a mask that visually matches the desired raw mask more closely than the simplified approach. Table 2 details the shot count with the layout generated from the corresponding assist feature. The raw and simplified masks are fractured by Calibre.©,[40] As seen, our proposed algorithm decreases the shot count by more than 50% as compared to simplified assist features.

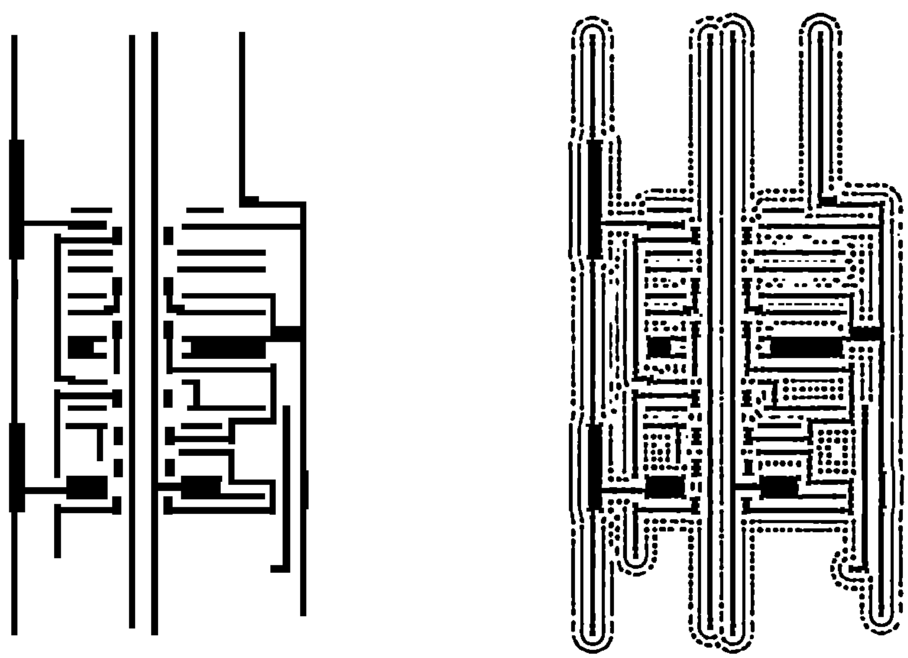

(a) (b)

Figure 2: Logic circuit: (a) Wafer target (b) Raw PIXbar™ assist features with edge-based OPC main features.

Table 2: Comparison of shot count for various assist features.

Raw Solution	Simplified Solution	Proposed Algorithm Solution
54,736	15,712	6,964

We verify the mask by comparing the edge placement error (EPE) of the simulated wafer images for the each mask. The histograms of the EPE for all three cases are shown in Fig. 4. The EPE is examined at nominal focus

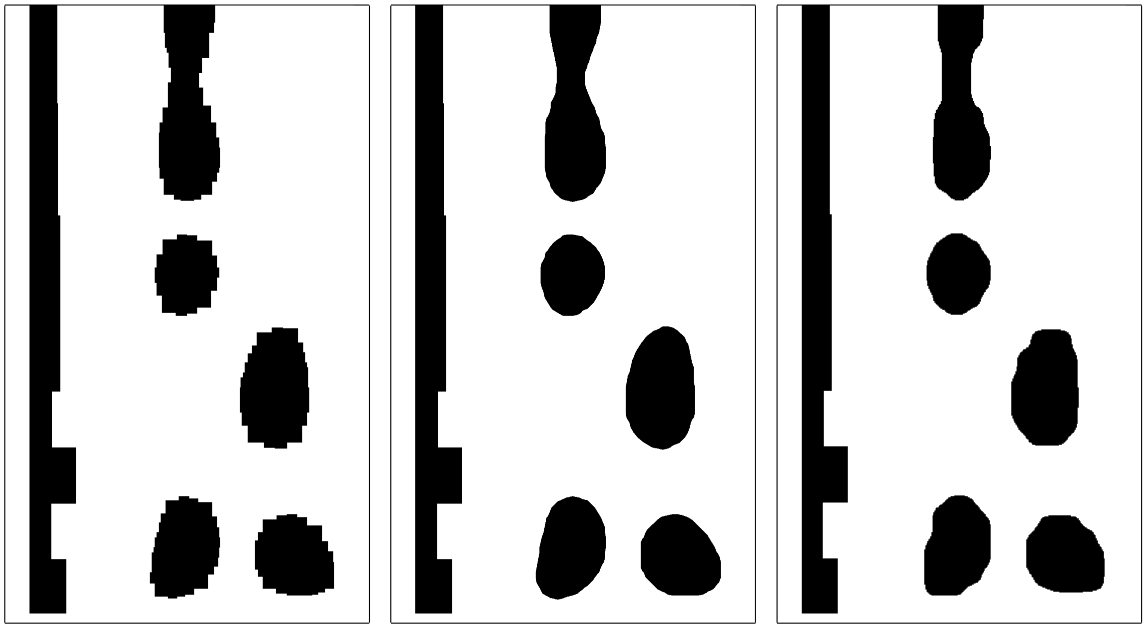

(a) (b) (c)

Figure 3: Comparison of masks for logic circuit: (a) Simple mask (b) Raw mask (c) Mask from proposed algorithm.

and +75nm, -50nm defocus. The choice of -50nm defocus is selected as our focus plane was placed at +50nm relative to the resist. As we use an ideal resist, the optical model is symmetric about the resist stack so defocus below -50nm is not relevant.

To compute the EPE, all edges of the polygons are partitioned into fragments smaller than 1μm in length. Then the EPE is measured at various points along the fragment and the average is recorded for each fragment. In the histogram, the x-axis corresponds to the average EPE for an edge fragment while the y-axis corresponds to the number of fragments with an average EPE in that range. At nominal focus and at -50nm defocus the EPE histograms are almost the same for all three layouts. However, at +75nm defocus the raw mask has slightly fewer fragments with an average EPE greater than 5nm in magnitude, as compared with simple mask and the mask from our proposed algorithm. In comparing the simple mask and the mask from our proposed algorithm we see that the simple mask has increased number of fragments with an EPE of -20nm. Otherwise, it is extremely difficult to distinguish the three masks by EPE, even at defocus. We conclude that our proposed algorithm closely matches the Calibre© edge placement error for the simple mask with a significantly lower shot count.

Fig. 5 shows histograms of the types of shots our algorithm generates. Despite limiting the shot sizes in our initial dictionary, Figs. 5 (a)-(d) show existence of shots of all sizes and aspect ratios. We notice that in Fig. 5 (c) many of the shots are maximal in length in the y-dimension; this is due to the layout being vertically oriented. Finally, Figs. 5 (e)-(f) show most of the shots are near the maximum allowed dosage of 5 which is a characteristic of the greedy dose selection.

Fig. 6 provides an example of the output of our proposed algorithm; it shows the desired mask target, the simulated mask generated by our algorithm, the difference between our simulated mask the the target mask, and the shot locations. As seen, the difference is quite insignificant indicating the high quality of approximation. Another interesting feature of our proposed algorithm is that while it allows for shot overlap, it does not require shots to be adjacent. In fact, we see that the far shot on the left is completely isolated. Despite this, the approximated feature is quite close to the desired target.

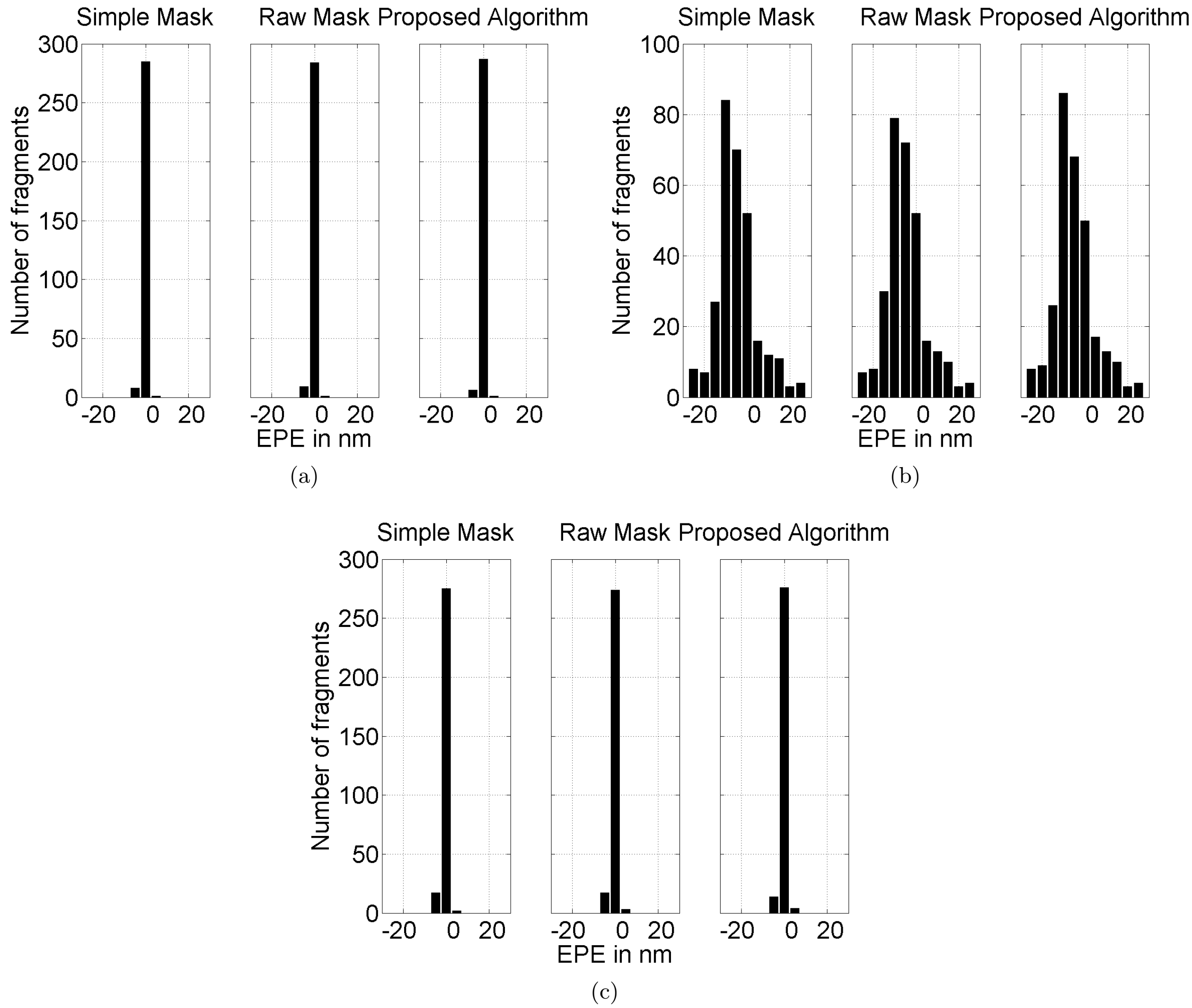

Figure 4: Edge placement error across defocus: Histogram of EPE at (a) nominal focus, (b) +75nm defocus (c) -50nm defocus.

5.2 Contact Layer

Next we consider the contact layer of the SRAM chip at the 45nm technology node. The contacts are all square with side length of 70nm. We use the same wafer simulation conditions as in Table 1.

To test this layout we follow the same approach outlined earlier to evaluate our approach. Namely, we use PIXBar^{TM} to generate three types of assist features and then run edge-based OPC with the assist features on the main feature. The target wafer image and desired mask from optimization are shown in Fig. 7. A comparison of the three types of resulting masks is shown in Fig. 8. As seen, the mask from our proposed algorithm visually matches the raw mask more closely than the simplified mask.

Table 3 details the shot count for each type of layout and fracturing. The raw and simplified masks are fractured by Calibre© while the last column is the raw mask fractured by our performed algorithm. As seen our proposed algorithm achieves a 60% reduction in shot count as compared with using simplified features.

As the circuit consists of contacts, we use the area ratio of the vias as the wafer fidelity metric. We examine the area ratio between the simulated contours and a smooth version of the desired contours generated using

Table 3: Comparison of shot count for various fracturing.

Raw Solution	Simplified Solution	Proposed Algorithm Solution
45,670	13,157	5,168

Calibre© OPCVerify™. This is done as the limitations of the optical system make printing a perfect square impossible. Fig. 9 shows histograms that evaluate area ratio for each contact. Again, this is done at nominal focus and at +/-40nm defocus. At nominal focus we notice that the area ratio of the wafer generated from the mask from our proposed algorithm performs competitively with the wafers generated by both simple and raw masks. At positive defocus and negative defocus the mask from our proposed algorithm clearly outperforms the simple mask with a greater number of contacts having area ratio near one. The same data suggest the mask from our proposed algorithm almost matches the raw mask in performance at positive defocus by only having fewer contacts in the highest bin. At negative defocus the mask from our proposed algorithm actually outperforms the raw mask with slightly more contacts clustered around one. We conclude that our proposed algorithm generates a mask that is competitive, in terms of wafer quality, with both the simple and raw masks but also achieves it with a 60% decrease in shot count relative to the simple mask.

6. CONCLUSIONS AND FUTURE WORK

In this paper, we develop a novel model-based fracturing algorithm based on OSE algorithms. We demonstrate a shot count reduction of over 50% as compared with fracturing a simplified version of the pixel-based OPC. This is achieved with minimal impact on mask fidelity and image wafer quality. For a random logic circuit we see a minor shift in the EPE histogram while for a set of vias we see that our contact area is very close to 1 and across defocus is close to the raw mask results.

In future work we plan to test the limits of our algorithm on smaller technology nodes in which pixel-based mask optimization techniques are even more important. We intend to explore the influence of mask writer parameters on our results and to further incorporate mask constraints into our algorithm. Finally, we plan to extend this work to non-rectangular shots such as trapezoids and triangles.

7. ACKNOWLEDGMENTS

We wish to express our gratitude to Vivek Singh of Intel for his part in initiating this line of research. We wish to acknowledge the contributions of the students, faculty, and sponsors of the Berkeley Wireless Research Center, in particular Brian Richards. Further, without the wafer layouts from STMicroelectronics we could not have tested the algorithms proposed. We wish to thank Yuri Granik and Emile Sahouria from Mentor Graphics for their critical help in working with the Calibre© software package. Finally, we express our thanks to Richard Lozes, Peter Buck, Jim DeWitt, and Ines Stolberg for many useful technical inputs on mask writers.

REFERENCES

1. A. B. Kahng, X. Xu, and A. Zelikovsky, “Yield- and cost- driven fracturing for variable shaped-beam mask writing,” in *Proc. 24th BACUS Symposium on Photomask Technology and Management*, pp. 360–371, Sep.(2004)
2. A. B. Kahng, X. Xu, and A. Zelikovsky, “Fast yield driven fracture for variable shaped beam mask writing”, *Proc. SPIE Int. Soc. Opt. Eng. 6283*, 62832R (2006)
3. N. Hiroomi, K. Moriizumi, K. Kamiyama, “A new figure fracturing algorithm for high quality variable-shaped EB exposure-data generation”, *Proc. SPIE, Kawasaki 1996*, 2793:398-409.
4. M. Bloecker, R. Gladhill, P. D. Buck, M. Kempf, D. Aguilar, R. B. Cinque, “Metrics to Assess Fracture Quality for Variable Shaped Beam Lithography”, *Proc. of SPIE Vol. 6349*, 63490Z (2006) .
5. C. Spence, S. Goad, P. Buck, R. Gladhill, R. Cinque, J. Preuninger, U. Griesinger, M. Bloecker, “Mask data volume: historical perspective and future requirements, *Proc. SPIE Int. Soc. Opt. Eng. 6281*, 62810H (2006)
6. A. Fujimura, I. Bork, T. Kiuchi, T. Komagata, Y. Nakagawa, K. Hagiwara and D. Hara, “Improvement of mask write time for curvilinear assist features at 22nm”,, *Proc. SPIE Vol. 7823*, 782307 (2010).
7. Christophe Pierrat and Ingo Bork, “Impact of model-based fracturing on e-beam proximity effect correction methodology”, Proc. SPIE 7823, (2010).
8. Christophe Pierrat, Larry Chau and Ingo Bork, “Mask data correction methodology in the context of model-based fracturing and advanced mask models“, Proc. SPIE 7973 (2010).
9. S. G. Mallat and Z. Zhang, “Matching Pursuits with Time-Frequency Dictionaries”, IEEE Transactions on Signal Processing, December 1993, pp. 3397-3415.
10. S. Jiang, X. Ma, A. Zakhor, “A recursive cost-based approach to fracturing”, Proc. SPIE 7973, 79732P (2011).
11. X. Ma, S. Jiang, A. Zakhor, “A cost-driven fracture heuristics to minimize external sliver length”, Proc. SPIE 7973, 79732O (2011).
12. N. Cobb, “Fast Optical and Process Proximity Correction Algorithms for Integrated Circuit Manufacturing,” Ph.D. Thesis, Department of Electrical Engineering and Computer Sciences, University of California, Berkeley, May 1998.
13. N. Cobb, ”Fast Mask Optimization for Optical Lithography,” Master’s Thesis, Department of Electrical Engineering and Computer Sciences, University of California, Berkeley, December 1994.
14. N. Cobb, A. Zakhor, M. Reihani, F. Jahansooz, and V. Raghavan, ”Experimental Results on Optical Proximity Correction with Variable Threshold Resist Model,” in SPIE Symposium on Optical Microlithography, Santa Clara, California, March 1997, vol. 3051, pp. 458-468.
15. N. Cobb, A. Zakhor, and E. Miloslavsky, ”Mathematical and CAD Framework for Proximity Correction,” in Proceedings of SPIE Symposium on Optical Microlithography, Santa Clara, CA, March 1996, vol. 2726, pp. 208-222.
16. N. Cobb and A. Zakhor, ”Fast Sparse Aerial Image Calculation for OPC,” in Proceedings of BACUS Symposium on Photomask Technology, Santa Clara, California, September 1995, vol. 2621, pp. 534-545.
17. N. Cobb and A. Zakhor, ”Fast, Low-Complexity Mask Design,” in Proceedings of the SPIE Symposium on Optical Microlithography, Santa Clara, California, February 1995, vol. 2440, pp. 313-327. [Postscript]
18. N. Cobb and A. Zakhor, ”Large Area Phase Shift Mask Design,” in Proceedings of SPIE Symposium on Optical Laser Microlithography VII, San Jose, California, March 1994, vol. 2197, pp. 348-360.
19. Vivek Singh, Bin Hu, Kenny Toh, Srinivas Bollepalli, Stephan Wagner and Yan Borodovsky, “Making a trillion pixels dance”, Proc. SPIE 6924, 69240S (2008); doi:10.1117/12.773248.
20. Yuri Granik, “Fast pixel-based mask optimization for inverse lithography”, J. Microlith., Microfab., Microsyst. 5, 043002 (Dec 13, 2006); doi:10.1117/1.2399537
21. R. Neff, and A. Zakhor, “Very Low Bit Rate Video Coding Based on Matching Pursuits” in Wavelet Image and Video Compression, edited by P. N. Topiwala, Kluwer Academic Publishers, 1998, Chapter 22, pp. 361-382.

22. P. Schmid-Saugeon and A. Zakhor, “Dictionary Design for Matching Pursuit and Appliation to Motion Compensated Video Coding” in IEEE Transactions on Circuits and Systems for Video Technology, Vol. 14, no. 6, June 2004, pp. 880 - 886.
23. C. De Vleeschouwer and A. Zakhor, “In loop atom modulus quantization for matching pursuit and its applications to video coding” in IEEE Transactions on Image Processing, Vol. 12, No. 10, October 2003, pp. 1226 - 1242.
24. X. Tang and A. Zakhor, “Matching Pursuit Multiple Description Coding for Wireless Video“, IEEE Transactions on Circuits and Systems for Video Technology, Vol. 12, No. 6, June 2002, pp. 566-575.
25. R. Neff and A. Zakhor, “Matching Pursuit Video Coding - Part 1: Dictionary Approximation“, IEEE Transactions on Circuits and Systems for Video Technology, Vol. 12, No. 1, January 2002, pp. 13-26.
26. R. Neff and A. Zakhor, “Matching Pursuit Video Coding - Part 2: Operational Models for Rate and Distortion“, IEEE Transactions on Circuits and Systems for Video Technology, Vol. 12, No. 1, January 2002, pp. 27-39.
27. R. Neff and A. Zakhor, “Modulus Quantization for Matching Pursuit Video Coding“, IEEE Transactions on Circuits and Systems for Video Technology, Vol. 10, No. 6, September 2000, pp. 895-912.
28. R. Neff and A. Zakhor, “Very Low Bit-Rate Video Coding based on Matching Pursuits,” in IEEE Transactions on Circuits and Systems for Video Technology, February 1997, vol. 7, no. 1, pp. 158-171. (Best Paper Award.)
29. P. Garrigue and A. Zakhor, “Atom Positioni Coding in a Matching Pursuit Based Video Coder“, VLBV workshop, Sardinia, Italy, September 2005, Book SeriesLecture Notes in Computer Science, Visual Content Processing andRepresentation, Springer Berlin / Heidelberg, Volume 3893, 2006, pp. 153 - 160.
30. T. Nguyen and A. Zakhor, “Matching Pursuits Based Multiple Description Video Coding for Lossy Environments” in International Conference on Image Processing 2003, Vol. 1, Barcelona, Spain, September 2003, pp.57-60. (invited paper)
31. C. D. Vleeschouwerand A. Zakhor, “Atom Modulus Quantization for Matching Pursuits Video Coding” in International Conference on Image Processing 2002, Rochester, New York, September 2002, Vol. 3, p. 681-684.
32. X. Tang and A. Zakhor, “Matching pursuits multiple description coding for wireless video” in Proceedings of the International Conference on Image Processing, Thessaloniki, Greece, October 2001, Vol. 1, p. 926-929.
33. R. Neff and A. Zakhor, “Dictionary Approximation for Matching Pursuit Video Coding” in Proceedings of the International Conference on Image Processing, Vancouver, Canada, September 2000, Vol. 2, pp. 828-831.
34. E. Miloslavsky and A. Zakhor, “Rate Control for Layered Video Compressing Using Matching Pursuits,” in Proceedings of the International Conference on Image Processing, Kobe, Japan, October 1999, vol. 2, pp. 357-361.
35. R. Neff and A. Zakhor, “Adaptive Modulus Quantizer Design for Matching Pursuit Video Coding,” in Proceedings of the International Conference on Image Processing , Kobe, Japan, October 1999, vol. 2, pp. 81-85. (Best Paper Award.)
36. R. Neff, T. Nomura, and A. Zakhor, “Decoder Complexity and Performance Comparison of Matching Pursuit and DCT-based MPEG-4 Video Codecs,” in Proceedings of the IEEE International Conference on Image Processing (ICIP), Chicago, IL, 4-7 October 1998, vol. 1, pp. 783-787.
37. R. Neff, A. Zakhor, and M. Vetterli, “Very Low Bit Rate Video Coding Using Matching Pursuits,” in Proceedings of SPIE Conference on Visual Communication and Image Processing, Chicago, Illinois, September 1994, vol. 2308, pp. 47-60.
38. R. Neff, “New Methods for Matching Pursuit Video Compression,” Ph.D. Thesis, Department of Electrical Engineering and Computer Sciences, University of California, Berkeley, December 2000.
39. P. Garrigues, “Atom Position Coding in a Matching Pursuit Based Video Coder“, Master’s Thesis, Department of Electrical Engineering and Computer Sciences, University of California, Berkeley, January, 2006.
40. http://www.mentor.com/

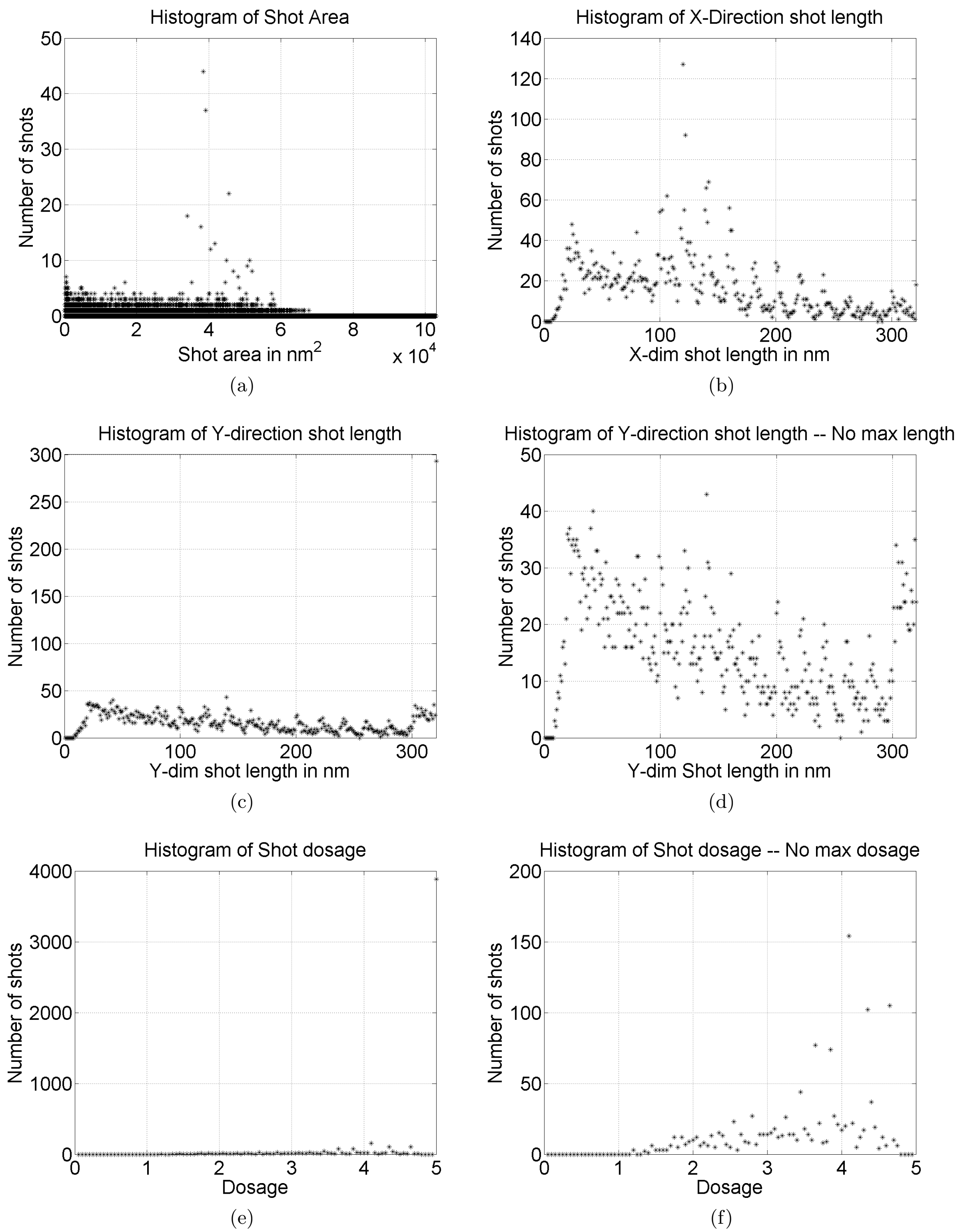

Figure 5: Shot distribution for random logic: Histogram of (a) area of shots (b) shot length in x-dimension (c) shot length in y-dimension (d) shot length in y-dimension maximum shot length excluded (e) shot dosage (f) shot dosage with maximum dosage excluded.

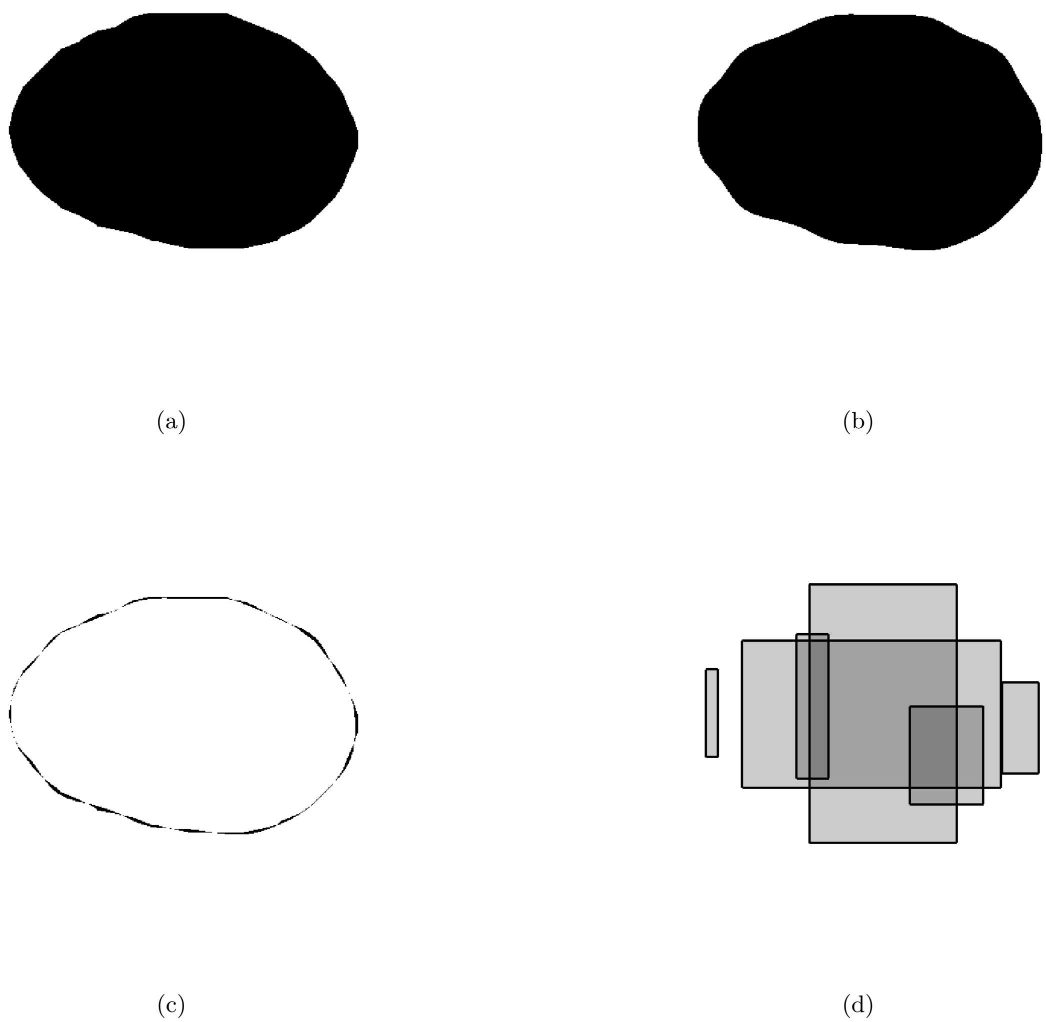

Figure 6: An example of the performance of our algorithm on an assist feature: (a) target feature (b) approximated feature (c) Difference between target and approximatioin (d) shot locations.

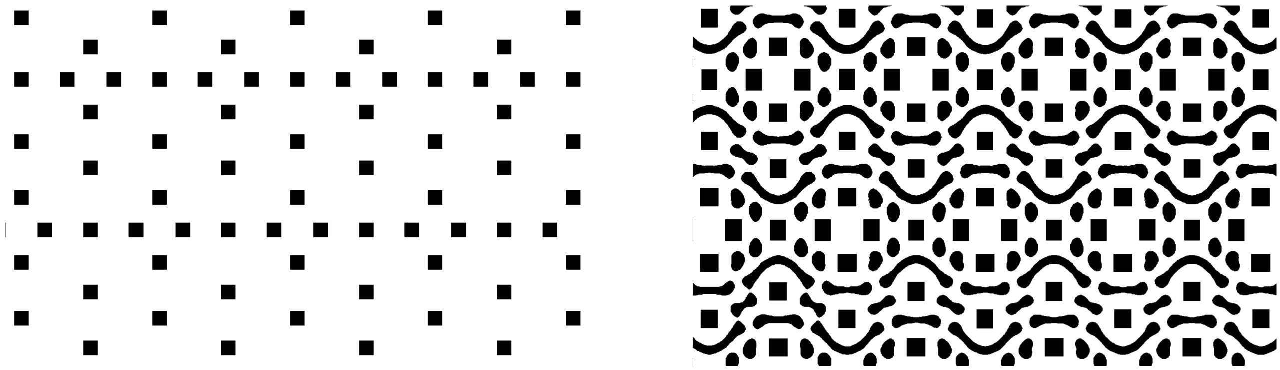

(a) (b)

Figure 7: (a) Target wafer image (b) Raw PIXbar$^{\mathrm{TM}}$ assist features with edge-based OPC main features.

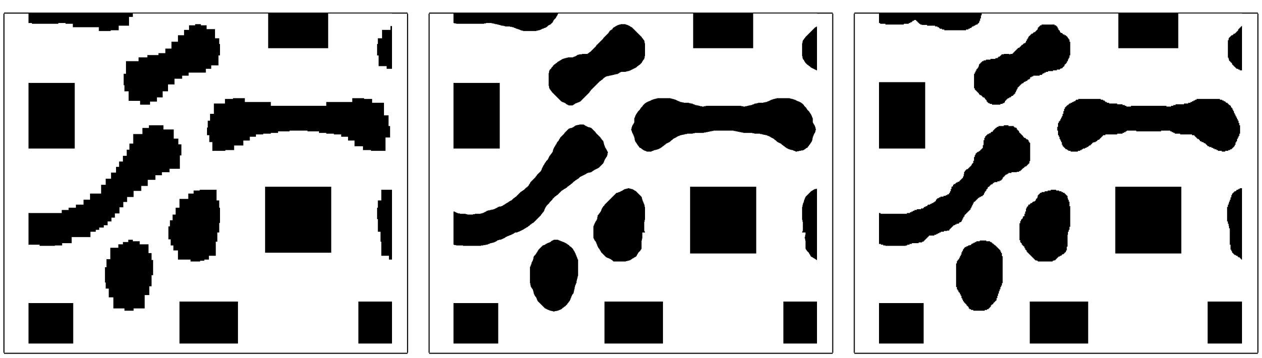

(a) (b) (c)

Figure 8: Comparison of masks for logic circuit: (a) Simple mask (b) Raw mask (c) Mask from proposed algorithm.

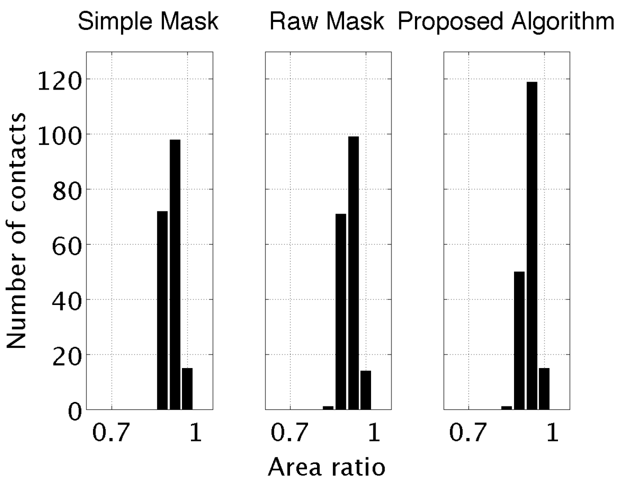

(a)

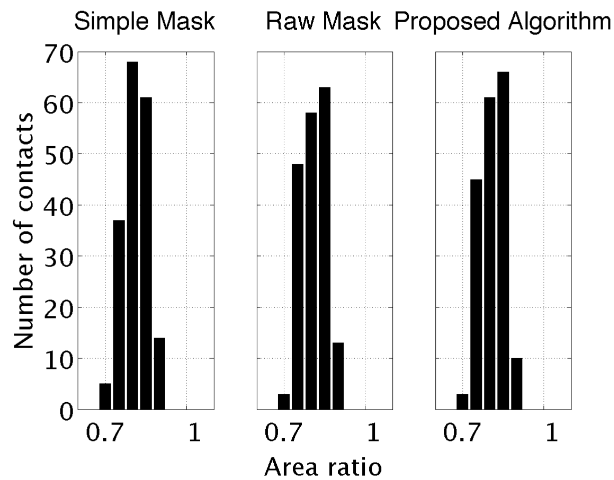

(b)

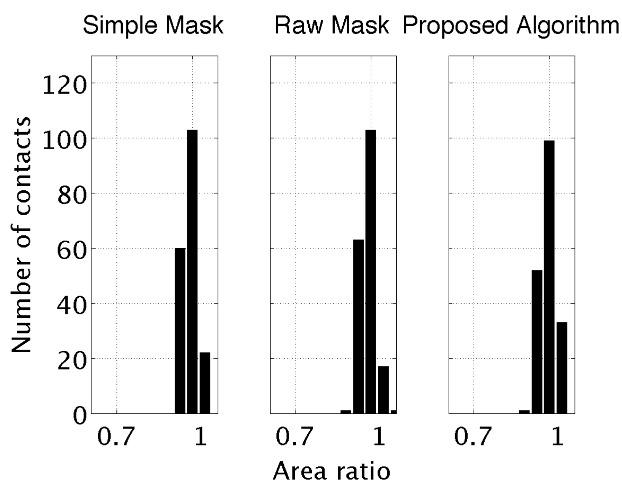

(c)

Figure 9: Histogram of area ratio at (a) nominal focus (b) +40nm defocus (c) -40nm defocus.